University of Helsinki Report Series in Physics

HU-P-D226

Quality Assurance of Gas Electron Multiplier Detectors

Timo Eero Hildén

Division of Elementary Particle Physics
Department of Physics
Faculty of Science
University of Helsinki
and
Helsinki Institute of Physics
Helsinki, Finland

Academic Dissertation

To be presented for public criticism, with the permission of the Faculty of Science of the University of Helsinki, in the auditorium LS2 of the Chemicum building, A.I. Virtasen aukio 1, on Thursday, March 5th, 2015, at 12.00 o'clock.

Helsinki 2015

Supervisor:

Prof. Risto Orava, Ph.D.
Department of Physics
University of Helsinki
Finland

Reviewers:

Prof. Ari Jokinen
Department of Physics
University of Jyväskylä
Finland

Dr. Peter Cwetanski
Nagravision SA
Switzerland

Opponent:

Prof. Richard Brenner, Ph.D.
Department of Physics and Astronomy
Uppsala University
Sweden

Cover image:
A rendered image of a Garfield++ simulation of an avalanche caused by a single electron drifting into a GEM hole. The tracks of electrons are drawn in white and the tracks of the ions are drawn in yellow lines.

Report Series in Physics HU-P-D226
ISSN 0356-0961
ISBN 978-951-51-0582-0 (printed version)
ISBN 978-951-51-0583-7 (electronic version)
`http://ethesis.helsinki.fi`
Unigrafia

Helsinki 2015

Abstract

Gas Electron Multiplier (GEM) detectors are special of position sensitive gas filled detectors used in several particle physics experiments. They are capable of sub-millimeter spatial resolution and energy resolution (FWHM) of the order of 20%. GEM detectors can operate with rates up to 50 kHz/mm^2, withstand radiation excellently and can be manufactured up to square meter sizes.

This thesis describes the Quality Assurance (QA) methods used in the assembly of 50 GEM detectors for the TOTEM T2 telescope at the LHC at CERN. Further development of optical QA methods used in T2 detector assembly lead into development of a unique large-area scanning system capable of sub-μm resolution. The system, its capability and the software used in the analysis of the scans are described in detail.

A correlation was found between one of the main characteristics of the detector, the gas gain, and the results of the optical QA method. It was shown, that a qualitative estimation of the gain can be made based on accurate optical measurement of the microscopic features of the detector components. Ability to predict the performance of individual components of the detectors is extremely useful in large scale production of GEM based detectors.

Acknowledgements

First of all, I would like to thank professor Risto Orava for the unforgettable experience of working as a member of the TOTEM experiment at the LHC. I had a chance to conduct my studies as part of an international collaboration and also the exceptional opportunity to follow a particle physics experiment from the conception to a narrative conclusion as the "Long Shutdown 1" began in 2013. I am grateful for his support and confidence in me during my studies.

I would also like to express my gratitude to professor Ari Jokinen and Dr. Peter Cwetanski for reviewing my thesis. I'm especially thankful of their alacrity and expertise in providing me the feedback I needed to finish my thesis in a timely manner.

My deep gratitude goes also to Dr. Erik Brücken and Dr. Eija Tuominen for reading my thesis and providing important suggestions on how to improve it.

The Detector Laboratory of Helsinki Institute of Physics and the University of Helsinki made my work possible. I am grateful of the help of my colleagues, especially Jouni Heino, Dr. Matti Kalliokoski, Kari Kurvinen and Rauno Lauhakangas, for their invaluable help. I would also like to thank Dr. Eraldo Oliveri from the TOTEM experiment and the RD-51 collaboration for his broad insight into gas filled detectors.

My graduate studies were funded by the Helsinki Institute of Physics. Additional funding by Magnus Ehrnrooth Foundation, Waldemar von Frenckell Foundation and Academy of Finland were also instrumental in letting me finish my work.

Finally, I want to thank Päivi, Miro, Jooa, Tome, Minea and Selia for support, encouragement and, most importantly, patience.

List of Publications

I Hilden, T., 2009. The TOTEM T2 GEM detector assembly and quality assurance. J. Instrum. 4. doi:10.1088/1748-0221/4/11/P11020

II Kalliokoski, M., Hilden, T., Garcia, F., Heino, J., Lauhakangas, R., Tuominen, E., Turpeinen, R., 2012b. Optical scanning system for quality control of GEM-foils. Nuclear Instruments and Methods in Physics Research Section A: Accelerators, Spectrometers, Detectors and Associated Equipment 664, 223 – 230. doi:10.1016/j.nima.2011.10.058

III Kalliokoski, M., Hilden, T., Garcia, F., Heino, J., Lauhakangas, R., Tuominen, E., Turpeinen, R., 2012a. Analyzing GEM-foil properties with an optical scanning system. Journal of Instrumentation 7, C02059. doi:10.1088/1748-0221/7/02/C02059

IV Kalliokoski, M., Hilden, T., Garcia, F., Lauhakangas, R., Numminen, A., 2010. Study of GEM-foil defects with optical scanning system, in: 2010 IEEE Nuclear Science Symposium Conference Record (NSS/MIC). Presented at the 2010 IEEE Nuclear Science Symposium Conference Record (NSS/MIC), pp. 1446–1449. doi:10.1109/NSSMIC.2010.5874011

V Hilden, T., Brücken, E., Heino, J., Kalliokoski, M., Karadzhinova, A., Lauhakangas, R., Tuominen, E., Turpeinen, R., 2014. Optical quality assurance of GEM foils. Nuclear Instruments and Methods in Physics Research A, (2014), ISSN 0168-9002, doi:10.1016/j.nima.2014.10.015

VI Karadzhinova, A., Hildén, T., Heino, J., Berdova, M., Lauhakangas, R., Garcia, F., Tuominen, E., Kassamakov, I., 2013. Calibration of high-aspect ratio quality control optical scanning system. Proc. SPIE 8839, Dimensional Optical Metrology and Inspection for Practical Applications II, 88390G (September 6, 2013); doi:10.1117/12.2024100

Author's Contribution

Publication I: The TOTEM T2 detector assembly and quality assurance
This paper describes the quality assurance procedure used in the mass production of the 50 GEM detectors built at Helsinki for CERN TOTEM T2 telescope. The author was part of the TOTEM T2 QA team. He was especially responsible for the electrical testing and the optical scanning of the GEM foils. He also wrote the paper.

Publication II: Optical scanning system for quality control of GEM foils
This paper describes the high precision optical scanning system built at Helsinki for the quality assurance of GEM foils. The design and performance of the system is described. The author took part in the design, commissioning and tuning of the system. He also partially wrote the paper.

Publication III: Analyzing GEM-foil properties with an optical scanning system
This paper describes the first analysis results of a GEM foil with the Helsinki optical scanning system. The author took part in the work, especially in the image analysis of the scans. He participated in the writing process of the paper.

Publication IV: Study of GEM-foil properties with optical scanning system
This paper describes a study on the effects of and the evolution of etching defects in GEM foils, utilizing the Helsinki optical scanning system. The measurements were done with a GEM detector built using foils with known defects. The author of this thesis took part in the work and participated in the writing process of the paper.

Publication V: Optical quality assurance of GEM foils
This paper discusses the analysis software developed for the quality assurance of GEM foils. This software was used to analyze GEM foil images taken with the Helsinki optical scanning system. The quality of the analysis and the correlation between the size distribution of the GEM holes and the performance of the foils are discussed. The author of this thesis is responsible for the development of the analysis software. He also wrote the paper.

Publication VI: Calibration of high-aspect ratio quality control optical scanning system
This paper describes the calibration of the Helsinki optical scanning system using calibration samples. The author of this thesis was responsible for the scanning software, part of the analysis and tuning of the system. He also took part in the writing of the paper.

Contents

Abbreviations

ALICE	A Large Ion Collider Experiment
CERN	Conseil Européen pour la Recherche Nucleaire
CMS	Compact Muon Solenoid
COMPASS	COmmon Muon Proton Apparatus for Structure and Spectroscopy
dpi	dots per inch
FAIR	Facility for Antiproton and Ion Research
FWHM	Full Width at Half Maximum
GEM	Gas Electron Multiplier
IP5	Interaction Point 5
LHC	Large Hadron Collider
lp/mm	line-pairs per millimeter
MICROMEGAS	MICRO MEsh GAseous Structure
MPGD	Micro Pattern Gas Detector
MSGC	Micro-Strip Gas Counter
MWPC	Multi-Wire Proportional Counter
OSS	Optical Scanning System
QA	Quality Assurance
ROB	Read Out Board
Super-FRS	Super-FRagment Separator
TOTEM	TOTal Elastic and diffractive cross section Measurement
TPC	Time Projection Chamber

CHAPTER 1

Introduction

Gas Electron Multiplier (GEM) detectors [**1**], along with a number of other Micropattern Gas Detectors (MPGD), are a rapidly advancing technology in the field of charged particle detection. GEM detectors can be constructed in up to square meter sizes, have been shown to have good rate capacity and radiation tolerance and can reach spatial resolution of less than 100 μm [**2**]. They are challenging solid-state detectors in many applications, due to their significantly lower cost per surface area unit.

Following the introduction of GEM detectors, wide range of applications have been devised for them. GEM detectors have been used to detect charged particles, hard gammas, soft x-rays, uv, visible light, neutrons etc. The proposed applications range from particle and nuclear physics experiments and medical physics to detectors used in border security. For several examples, see references [**4**, **5**].

The Large Hadron Collider (LHC) at CERN alone has two experiments [**6**, **7**], utilizing GEM detectors. Several new detector systems are currently being designed as upgrades to the existing systems for the LHC after it is upgraded to higher luminosities [**8**, **9**]. With the new GEM detectors being proposed for LHC, and for other international physics experiments [**10**, **11**], a trend towards bigger mass productions of GEM detectors with large active area can be seen.

GEM technology is undergoing a gradual change from experimental to routinely accepted technology. There is a serious push to launch commercial manufacturing of the components. The commercialization process, requires high yield manufacturing in large volumes. Thus, quality assurance methods also need to be developed with the change from small scale production to industrial scale manufacturing.

The assembly of the GEM detectors of the CERN TOTEM T2 telescope and other GEM related activities in the Detector Laboratory of University of Helsinki and Helsinki Institute of Physics have led to the development of unique optical Quality Assurance (QA) methodology. This has been the main subject of the author during his studies in the Helsinki research group.

This thesis describes the quality assurance methods used in the assembly of the TOTEM T2 GEM detectors. The techniques used in the large area optical scanning of

GEM foils that were later developed for the mass production of FAIR Time Projection Chamber (TPC) detectors [**11**] and the upcoming upgrade of the ALICE TPC [**8**] are also described. The background and operating principles of GEM detectors are described in Chapter 2. Chapter 3 presents the TOTEM T2 detector and the quality control measures used in the T2 GEM detector assembly. The optical scanning system developed for GEM foil characterization is discussed in Chapter 4. Finally, in Chapter 5, the significance of optical quality assurance procedures for mass production of GEM detectors is briefly discussed.

CHAPTER 2

Gas Filled Detectors

1. Principles of Gas-Filled Detectors

The first gas-filled detector was the proportional counter, invented in 1908 by Ernst Rutherford and Hans Geiger [**12**]. Proportional counter is a gas-filled tube with a thin anode wire stretched along its axis. The tube itself acts as a cathode and is usually held at ground potential. When a high voltage is applied to the anode, a cylindrically symmetric electric field is created in the detector volume collecting electrons released by the ionizing radiation.

A charged particle traveling through the gas volume of the detector will ionize the gas atoms along its track. Most of the scattering events are low energy interactions knocking electrons off molecules on the path of the incident particle. The number of the primary electron-ion pairs produced by the traversal of the particle is proportional to its energy, if the particle is fully stopped within the gas volume. If not, it is dependent on the stopping power of the measurement gas and the track length.

Photons can interact with the gas via photoabsorption or Compton scattering, both releasing an electron, which can in turn ionize the gas as described above. Due to low density of the gas, the radiation length of x-rays is long compared to typical dimensions of gas-filled detectors. Full efficiency cannot usually be obtained within the gas volume of the detector. Gas-filled detectors have been, however, used as x-ray detectors since the introduction of the proportional counter.

In a proportional counter, the signal from the primary ionization is amplified by avalanche multiplication of electrons drifting into high electric field near the wire. In high electric field, the electrons are accelerated sufficiently between successive collisions to produce further ionization. The original and all the secondary electrons drift onward with more ionizing collisions on their path, creating an exponentially growing avalanche of electrons. Charge multiplication of the order of 10^4 - 10^5 is easily achievable, enabling the detection of keV-scale signal with simple electronics. A simulation of an avalanche caused by single electron in a proportional chamber is shown in Figure 2.1.

The gas volume around the wire where avalanches are possible is extremely small compared to the full active volume of the proportional chamber so that each primary electron can be thought to undergo full avalanche multiplication. The signal from a proportional counter is thus proportional to the energy left in the gas volume by the ionizing particle, hence the name.

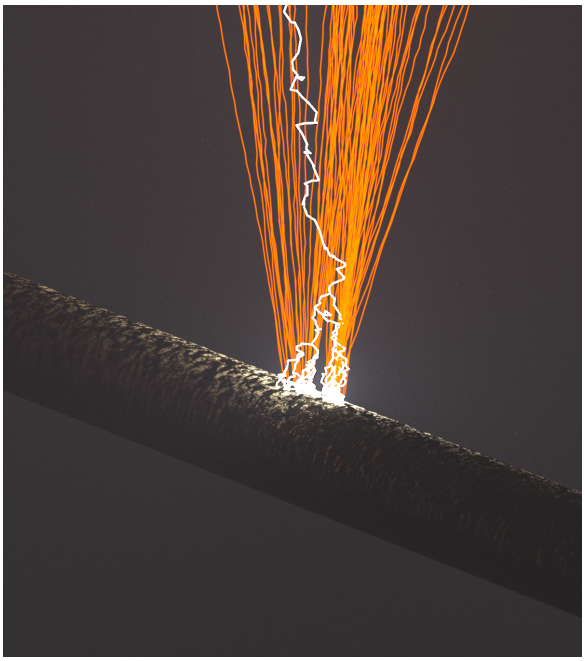

FIGURE 2.1. A Garfield++ [**13**] simulation of a single electron avalanche in a proportional chamber. The tracks of the electrons are drawn in white and the tracks of the ions in orange.

The basic principle of operation of gas-filled detectors has remained the same since the invention of the proportional chamber, with the exception of the ionization chamber, which is a gas-filled detector in which the direct current induced by ionizing radiation is measured.

Noble gases, used as measurement gas in gas detectors, have excitations emitting photons which can release electrons from the materials of the detector through the photoelectric effect. These electrons would then pass through the detector causing spurious pulses. The effect can be eliminated by adding another, often molecular, gas to the measurement gas. The purpose of this quenching gas is to absorb the photons emitted by the excitations of the noble gas component.

After the initial ionization, the electron-ion pairs start to drift along the electric field. While drifting, they undergo collisions with the molecules of the gas. During the drifting, the electrons deviate from the field lines through these collisions. The result is a drift length dependent uncertainty on their position, or diffusion. The cross-section

of elastic collisions contributes to the magnitude of the diffusion and to the mobility of the electrons and ions. The spatial and timing resolutions of gas filled detectors are defined by the mobility and diffusion in the gas. The composition of the gas defines the amount of primary ionization, the diffusion characteristics and the mobility of the ions and electrons.

Typically, the signal is formed in the readout electrodes by induction caused by the traversal of ions and/or electrons in the electric field of the detector. Electrons drift very fast compared to the massive ions. In proportional chambers, where the signal is mainly produced by the drift of ions from the anode wire, the rate capability is limited both by the slow rise time of the signal and because of the space-charge accumulating into the gas volume of the detector. In recent gas detector designs described in the next Section, this effect has been limited to some degree.

Gas-filled detectors are prone to aging, or the reduction of the performance of the detector with exposure to radiation. The aging effect can be attributed to polymer growth on electrodes in the vicinity of the avalanches, e.g. the anode wire of the proportional chamber. Organic molecules break down in the conditions of avalanche and may subsequently polymerize to nearby surfaces. This polymer buildup during the operation of the detector is strongly affected by the impurities of the gas [**14**]. Great care is to be taken with the choice of the detector materials, as some substances can release harmful compounds in to the gas. This phenomenon, called outgassing, can contribute strongly to the aging of the detector.

Gas-filled detectors are also prone to electric discharges, when the avalanche size surpasses the critical Raether limit (see [**15**] and references within). In a discharge the electric rigidity of the fill gas breaks down leading to streamer formation, which will short circuit the electrodes of the detector. Strong local disturbances in the electric field can have strong influence on the probability of the discharge formation.

2. Micropattern Gas Detectors

The proportional counter has been widely in use for nearly a century. In 1969, a significant improvement, the Multi Wire Proportional Counter (MWPC), was developed by G. Charpak [**16**]. A MWPC is essentially a row of anode wires within a single detector chamber. Each wire of the MWPC acts as an independent proportional counter. The MWPC made it possible to achieve larger coverage and better localization of tracks in high energy physics experiments.

The MWPC was the most commonly used gas filled detector until late eighties when the Micro-Strip Gas Counter (MSGC) was invented [**17**]. The MSGC is a structure, where alternating cathode and anode strips on an insulating substrate provide the

localized high field for avalanche formation. The advantage of MSGC over traditional MWPC is the fast cleanup of ions by the cathode strips close to the avalanche. Most of the ions created in the avalanche are collected by the nearest cathode strips instead of drifting through the drift volume of the detector. The rate capability of MSGC is orders of magnitude higher than that of MWPC, reaching MHz/mm2.

The MSCG has, however, inherent tendency to surface discharges between the closely spaced strips, which are potentially destructive to readout electronics and the delicate anode structure. Regardless of two decades of use and research, the problems with the MSGC are still not fully overcome.

It took a decade after MSGC for new types of MPGD detectors to emerge. Two of the most prominent types are the Micro Mesh GAseous Structure (MICROMEGAS) [**18**] and the GEM. Both detector types have spatial resolution, operational stability and radiation hardness beyond those of the previous generations of gas-filled detectors. The new MPGD detectors can be seen as low cost alternative to solid state detectors in applications where spatial resolution of hundreds or several tens of μm is sufficient.

In a MICROMEGAS detector, depicted in Figure 2.2, a fine metal mesh is fixed on insulating pylons very close to the readout plane, typically of the order of 100 μm. Avalanche formation starts in the region between the mesh and the readout plane, when sufficiently high voltage is applied between them. The field map of the area around the mesh, in Figure 2.2(b), shows how most of the field lines terminate to the wires of the mesh. A large fraction of the ions produced in avalanches between the mesh and the readout plane will drift into the wires, reducing significantly the ion backflow. A MICROMEGAS detector was used in Publication V as an independent detector coupled to a GEM foil.

A GEM foil is an insulating polyimide foil with metal electrodes on both sides. The foil is perforated with a dense pattern of small holes, typically 50 μm in smallest diameter and with a pitch of 140 μm. An electron microscope image of a GEM foil and a schematic illustration the geometry is shown in Figures 2.3 (a) and (b). The foil becomes an electron multiplier when the voltage between the electrodes is increased to allow avalanche formation inside the holes.

The shape of the holes of the GEM foil depends on the manufacturing technique. A standard GEM foil is manufactured by wet etching of the holes from both sides of the foil. This procedure produces double conical holes with significant difference between the diameters of the holes in the copper and in the middle of the polyimide. In so-called single mask production of the holes the etching is done from one side of the foil all the way through the foil in a single process. Thus, single mask foils have a

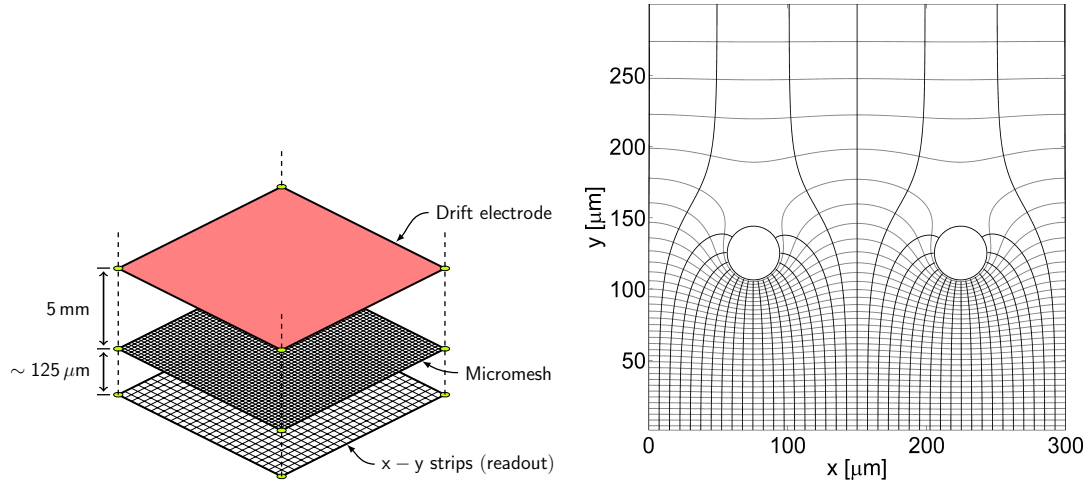

(a) (b)

FIGURE 2.2. A schematic illustration of a MICROMEGAS detector (a) and field map of the neighborhood of the mesh (b).

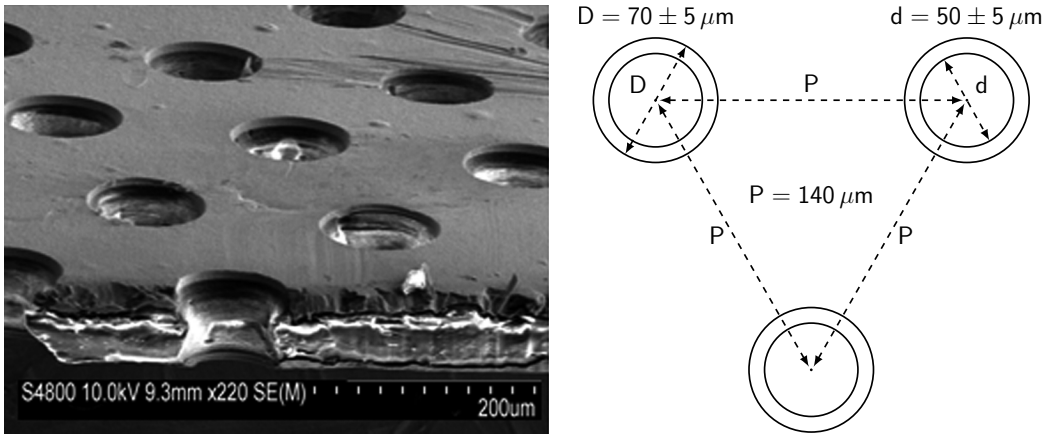

(a) (b)

FIGURE 2.3. SEM image of a GEM foil produced with the double mask technique.

conical cross section due to the processing. While the manufacture of single mask foils does not need the careful alignment of the masks on both sides of the foil, it produces foils that are asymmetric. The electric field maps of the different configurations of GEM foil geometry are shown in Figures 2.4(a) to (c).

The geometry of the GEM holes does affect the gas multiplication in the hole through several mechanisms, with the most obvious being the size of the hole. The field strength inside the hole increases as the diameter decreases, getting closer to that of the parallel plate field. The gain of the GEM foil follows this tendency up to a

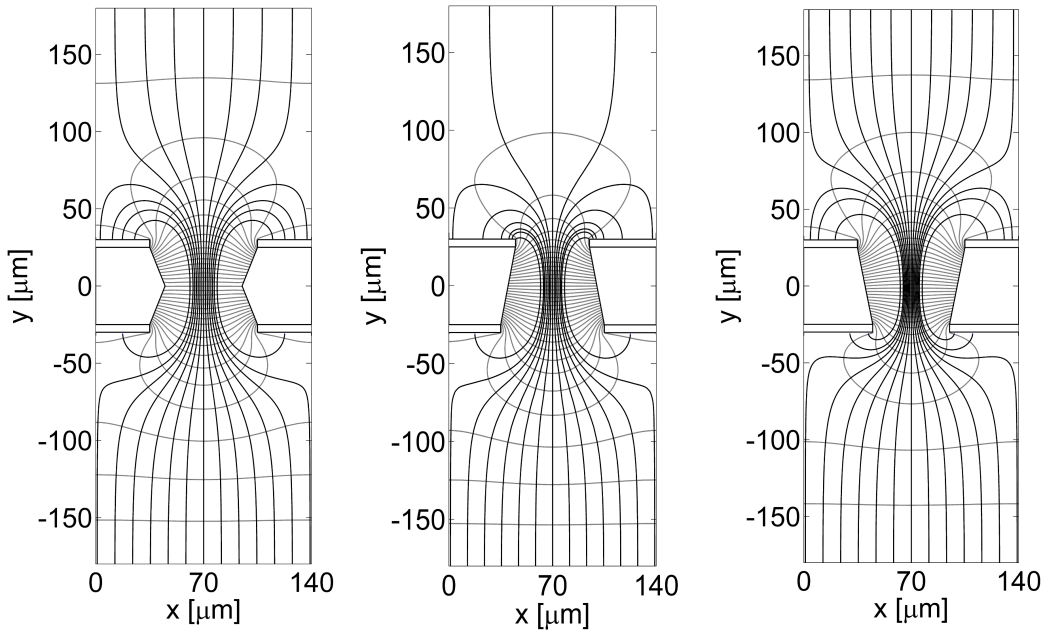

FIGURE 2.4. Electric field map of a double-mask GEM (left) and of a Single-mask GEM in both orientations (middle and right).

point, but the effect saturates as the diameter of the hole gets small enough. This is due to diffusion driving some of the electrons into the wall of the hole [**19**].

To allow the GEM foil to act as an electron multiplier, the electrons need to be collected in to the holes and subsequently extracted on the other side of the foil. The chance of electrons drifting into the holes reduces as the optical transparency of the foil is diminished by either increasing pitch or decreasing hole size. The optical transparency and the electric field setup influence the collection efficiency. The extraction efficiency depends on the shape of the holes, the diffusion of the electrons and, again, on the field setup. The effective gain of the foil, or the ratio of the electrons exiting the hole to the electrons entering the hole, can be significantly lower than the size of the avalanche due to electrons lost into the wall of the hole and the lower electrode.

An example of an avalanche induced by a single electron in a standard double conical GEM is shown in Figure 2.5. The tracks in the avalanche were simulated with GARFIELD++ toolkit [**13**]. In this particular avalanche 15 electron ion pairs are created by a single electron. Ten of the electrons (white tracks) are extracted from the hole, but only four ions (orange tracks) escape. An advantage of GEM detectors, and other MPGD detectors as well, is the suppression of the ions created in the avalanche. A significant portion of the drifting ions end up into the upper electrode of the foil, thus

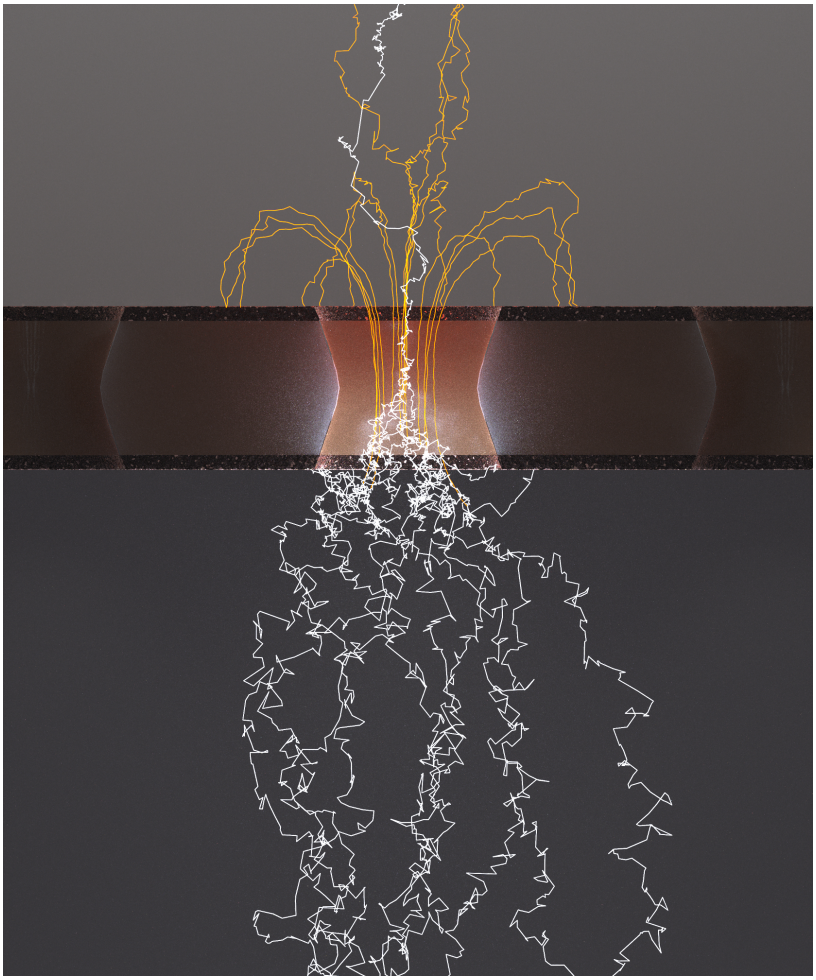

FIGURE 2.5. A Garfield++ simulation of an avalanche caused by a single electron drifting into the GEM hole. The tracks of the electrons are drawn with white and the tracks of the ions with orange lines.

reducing the space-charge accumulation in to the drift volume. The rate capability of the detector is increased proportionally.

Some of the electrons created in the avalanche inevitably end up in the insulating wall of the hole. The electrons and ions ending up to the insulator cause charge accumulation. Thus the electric field inside the hole changes until some equilibrium is achieved. The magnitude of the change of the field, and therefore the multiplication in the hole, depends on irradiation rate and the geometry of the hole. This effect, known as charging up, is difficult to simulate or measure, but some work on the field has been done recently, e.g. [**20**, **21**].

Another benefit of the GEM foil is the decoupling of the amplification stage from the readout. The readout is separated from the possible discharges during amplification, protecting the electrodes and the electronics, provided that the discharge does not

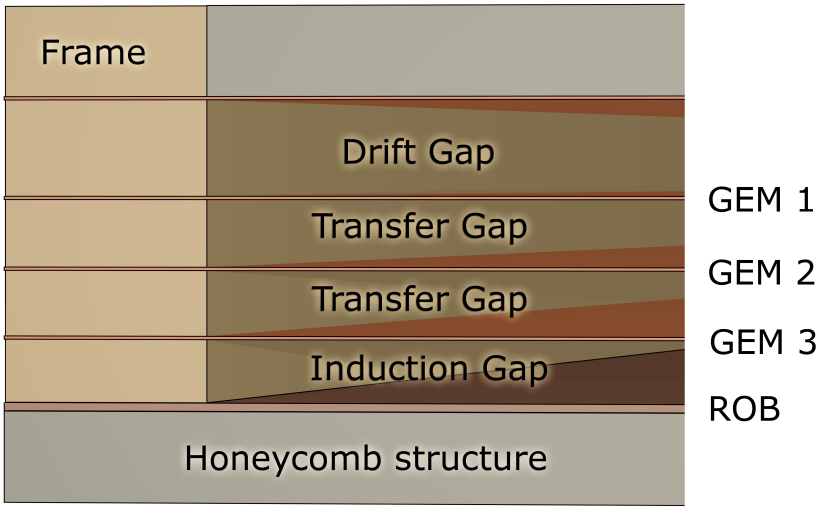

FIGURE 2.6. A schematic illustration of the TOTEM T2 triple GEM detector.

propagate out of the holes [**15**]. GEM foils can be stacked in series on top of each other, thus forming several multiplication stages as is shown in Figure 2.6. The electrons travel sequentially through the stack from the drift volume down to the readout plane. The discharge probability of the GEM detector can be reduced significantly by separating the multiplication to several low gain stages. This way maximum achievable gain can be increased without increasing the overall chance of damage to the detector.

The Raether limit still holds in GEM detectors, limiting the gain achievable in the lower stages of a multi-foil GEM detector, as the electron density increases. High gains, in the order of 10^4–10^5, can be achieved with asymmetric voltage division over the foils [**15**], where GEM foil voltage is reduced for the foils lower in the stack to keep discharge probability within acceptable region. An example of a triple GEM detector layout from TOTEM T2 GEM detectors can be seen in Figure 2.6. The size of the electron cloud from a multiple foil detector tends to be large due to diffusion and expansion to several holes during the drift. This effect can be useful to localize the centroid of the electron cloud when it is spread over several readout strips.

A multitude of MPGD detector derivatives have been introduced during the years after MSGC, GEM and MICROMEGAS were introduced. While varying a lot in details, the principle is the same, see e.g. reference [**4**].

CHAPTER 3

Quality Assurance of TOTEM T2 Telescope

1. TOTEM Experiment

The TOTEM experiment [**22**] at the LHC at CERN is dedicated to the measurement of the total proton-proton cross section, elastic scattering and soft diffractive processes over a large kinematic range. TOTEM consists of three detector systems placed symmetrically on both sides of the interaction point 5 (IP5): the T1 and T2 telescopes for the measurement of inelastic events at ≈ 9 and ≈ 14 m, respectively, from IP5 and the movable Roman Pot detectors for the measurement of beam-like protons at ≈ 147 and ≈ 220 m from IP5. Together, the three sub-detectors of TOTEM cover a pseudorapidity range of $3.1 < \eta < 6.5$ (T1 and T2) and $9 < \eta < 12$ (Roman Pots) on both sides of CMS. TOTEM, combined with the central coverage of CMS, covers more phase space than any other experiment at LHC.

This opens the door for a wide range of physics processes that can be studied. Elastic scattering, where the colliding protons remain intact after the collision, can be studied using the very forward Roman Pots. With the measurement of the inelastic rate and the differential cross section of elastic scattering, the total proton - proton cross section can be measured using the luminosity independent method. With the excellent forward coverage for charged-particle detection also single and double diffraction can be studied.

The inelastic detectors, T1 and T2, are important in the online selection of elastic and diffractive events. The signatures of the different processes are shown in Figure 3.1. General inelastic collisions can be studied with particles covering the whole eta phi phase space as shown in Figure 3.1(a). In elastic scattering, shown in Figure 3.1(b), the forward protons are detected with no activity in the rest of the detectors.

Diffractive processes make up a large fraction of the total cross section. In a diffractive process one or both of the colliding protons dissociate still retaining their quantum numbers. The diffractive system is visible in the inelastic detectors, as shown in Figure 3.1(c) and (d). Such a process is detectable as a forward system in either side with a leading proton in the opposite Roman Pot or as two forward systems with

a rapidity gap in between. A special type of diffractive process that can be studied is called the central exclusive production or double Pomeron exchange process as shown in Figure 3.1(e). Here a central massive system is produced with both colliding protons surviving the collision. In such a process there is a central system, rapidity gaps on both sides and the the leading protons in Roman Pots.

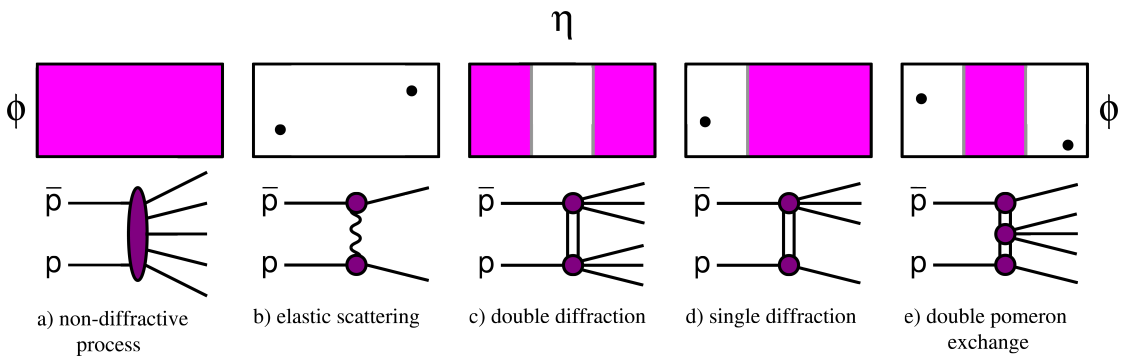

FIGURE 3.1. A schematic illustration of the signatures of different processes within the CMS + TOTEM acceptance.

2. TOTEM T2 Telescope

T2 telescope is one of the two inelastic detectors of TOTEM experiment. Whereas it is capable of measuring the inelastic rate for the total cross-section measurement with the luminosity independent method, it is also important for TOTEM by providing trigger information for elastic scattering and diffractive physics measurements by the Roman Pots.

The T2 is located symmetrically on both sides of IP 5 13.5 meters from the interaction point. The space for the detector is within the Hadronic Forward calorimeter of CMS. It is located in a region just behind a section where the beam pipe radius decreases from 300 mm to 55 mm. The beam pipe junction is thereby within the acceptance of T2 and is a source of secondary particles. The rate of secondary tracks due to the beam-gas interactions and the beam pipe is several times larger than rate of the primary tracks [**23**].

GEM technology was adapted to be used in the T2 telescope due to the high rate capability, mechanical robustness and good aging characteristics of GEM detectors. The choice of GEM detectors was further supported by the experience gained in the COMPASS experiment [**3**] over several years of operation in a high-rate environment. The COMPASS GEM design and quality assurance procedures were adopted as guidelines for the TOTEM T2 GEM detector production.

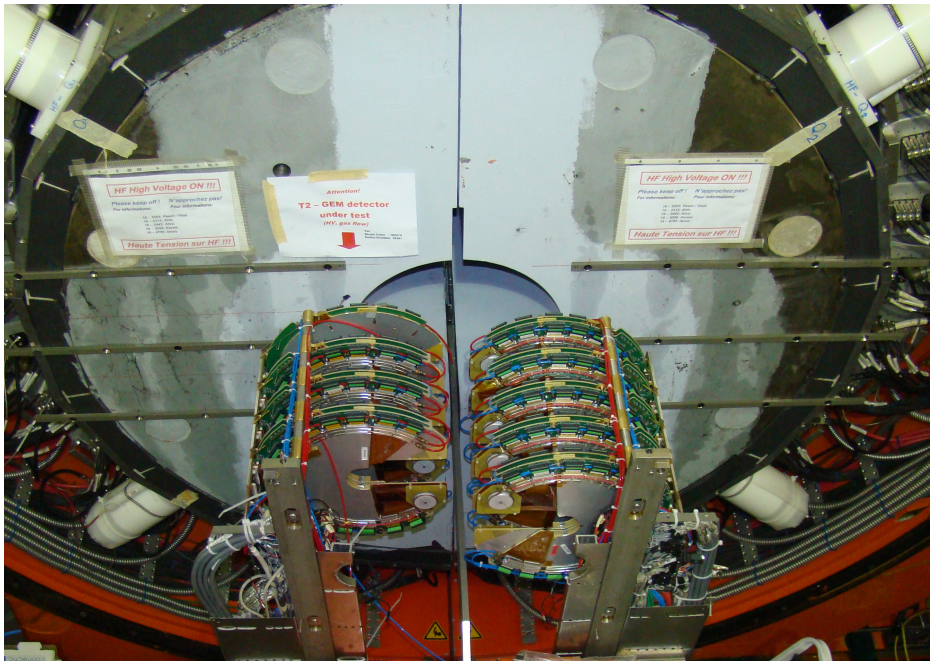

FIGURE 3.2. One side of the T2 telescope opened in the garage area of the CMS cavern.

The T2 telescope is placed symmetrically on both sides of CMS. One end of the telescope consists of two stacks of 10 semicircular detectors, called quarters, arranged around the beam pipe. The detectors, 40 in total, form ten planes of full azimuthal coverage on both sides of the IP5. Each detector element is semicircular, covering a slightly overlapping angle of 192° to allow for full efficiency within the border region of the two half-planes. Figure 3.2 shows quarters 1 and 2 spread apart in the garage area of the cavern. During installation, the quarters will be slid together around the beam pipe and then moved to the hole inside the Forward Calorimeter of the CMS.

To be able to trigger on tracks and provide necessary radial resolution for η measurements, the readout layout of T2 GEM detectors was chosen to be a combined pad and strip readout. The pads grant the trigger capabilities and azimuthal coordinates while the radial strips on top of the pads are used for radial coordinate measurement.

The readout board contains 256 concentric strips for measuring the radial coordinate. Because of high particle flux in the forward region the strips are divided into two halves, each covering 96° to relieve the average occupancy of the strips. A matrix of 1560 pads is divided into 65 columns of 24 pads radiating from the inner edge of the detector in roughly 3° increments. The readout channels are grouped into 13 Pad Sectors (PS), with 120 channels each, and four Strip Sectors (SS) with 128 channels each. The readout scheme is illustrated in Figure 3.3.

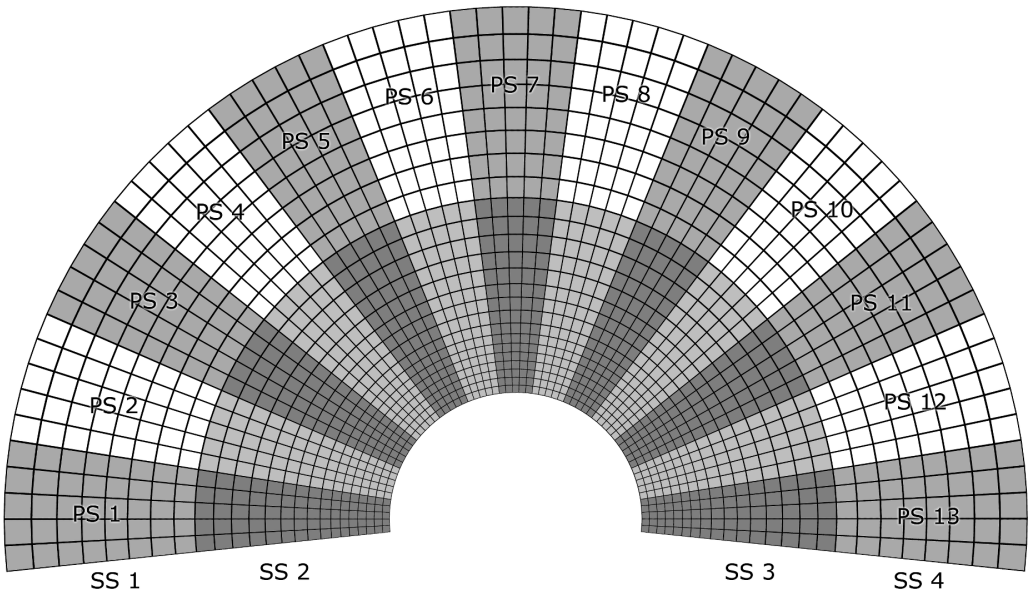

FIGURE 3.3. Readout map of TOTEM T2 GEM detector.

Due to the position of the T2 telescope, access to the detectors will become difficult once they are installed into IP5. All maintenance, whether for mechanics, electronics or detectors would be limited to the short winter shutdowns. Thus, the maintenance work must be done in cramped space and in short shifts due to the residual radiation. In practice, the maintenance of the T2 telescope will be limited to replacing any broken parts and performing minor fixes in-situ.

Furthermore, the harsh environment at 13,5 m adds severe criteria on the stability of the detector components. This is especially true with the quality of the GEM foils, the cooling system and the HV system. For these reasons the trustworthy and accurate performance of the detectors must be secured extremely carefully. Thus, the quality assurance of the detectors prior to installation is of utmost importance. All the T2 GEM detectors were assembled in the Detector Laboratory at Helsinki. Therefore there was a strong incentive in developing a sound quality assurance procedure for the assembly of the T2 GEM detectors.

3. Assembly of T2 Detectors

3.1. Assembly

The overview of the quality assurance procedure of the T2 telescope is described in Publication I. Here the aspects of the process that are important for our QA are discussed. The QA process had two primary objectives, firstly to maintain

and improve the quality of the assembly process and secondly to ascertain that the assembled detectors were up to the specifications defined by the TOTEM experiment.

A GEM foil is very sensitive to foreign material, such as dust or glue. Possible sources of such materials are tiny specks of dust left from the machining of detectors, various glues and varnishes of the assembly process and, of course, the assembly line environment. Special care was given to the cleanliness of the process throughout the assembly. All machined parts were thoroughly cleaned upon arrival and treated with a layer of conformal coating to bind the small dust that was inevitably left from the machining process. The full assembly process was conducted in class 100 and class 1000 cleanroom environment.

The assembly process itself was rather straightforward. Individual GEM foils were glued to frames and then the frames were glued together to form detector stacks. The stack was glued on top of the Read Out Board (ROB) to form the triple GEM chamber. After sealing of the chamber, the detectors could be brought out of the cleanroom environment for installing various connectors, cables etc. The assembly process was time consuming because of the series of testing phases and curing steps for the glue and the coatings used in the assembly.

3.2. Capacitance Measurement

Short circuits between the electrodes and broken strips in the detector ROBs can cause dead channels and unwanted noise. Thus, one of the most important tasks in the assembly of T2 was to test the read out channels. Often defective channels could be repaired by burning the short circuits off before the assembly of the ROB to the GEM-stack.

In addition to the visual inspection of the readout boards, a capacitance measurement of the readout channels was done. With 2072 channels per each GEM detector, and significant amount of time per measurement of single channel, manual testing would have been exceedingly time-consuming. Therefore, an automated capacitance measurement system was developed to measure the readout channel capacitances. The system consists of a computer controlled capacitance meter and a xyz-table. Each channel of the 17 sectors of a GEM detector was tested separately, pin by pin. Broken strips and short circuits between strips and pads could easily be observed from the measured capacitance values, as demonstrated in Figure 3.4.

3.3. Leakage Current Measurement

Currently the only way to get a quantitative measure of the performance of a GEM foil during the assembly is the leakage current measurement. In the leakage

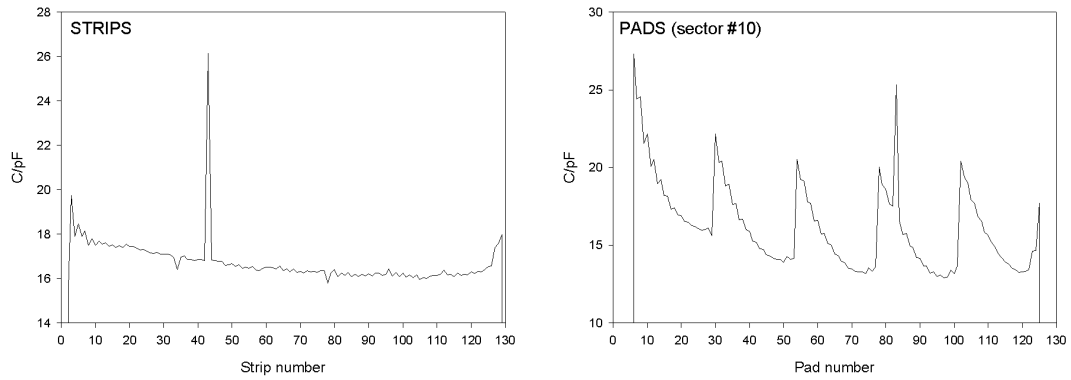

(a) (b)

FIGURE 3.4. Capacitance measurements indicating a short circuit between a strip and a pad that is clearly visible on top of the usual capacitance structure reflecting the readout board geometry.

current measurement, high voltage (HV) is applied to the electrodes of the foil and the resulting current is measured with a picoammeter. If there are sparks, seen as a transient current peak, or if the resistivity of the insulator is not high enough leading to higher than normal saturation current, the foil is suspected to not perform well. Some sparks are occasionally seen while the high voltage is ramped up, because in practice it is impossible to protect the foils from dust. The criterion for a good GEM foil in T2 was a stable period of at least 30 minutes under 500 V with no sparking and a stable saturation current of less than 0.5 nA.

The leakage current measurements were made three times for each HV sector of each foil: when the foils arrived into the Detector Laboratory, after they were framed and finally after the frames were glued together to form the detector stack. Testing the foils in several phases during the assembly was time consuming but allowed for an efficient way to notice mistakes in the assembly before the detector was fully assembled.

3.4. Optical Examination

It is clear that defects, such as incomplete or too strong etching of the holes or foreign matter on the foils are undesirable. Yet, the actual effects of these defects on the functioning and long term stability of GEM foils are poorly known. Some of these defects could be found out by optical examination of the foils, but just two T2 GEM foils were ever discarded due to visual inspection alone. There are no systematic studies available on the effects of the etching defects on the operation of GEM detectors. However a single study on the effects and evolution of the etching defects is found in Publication IV.

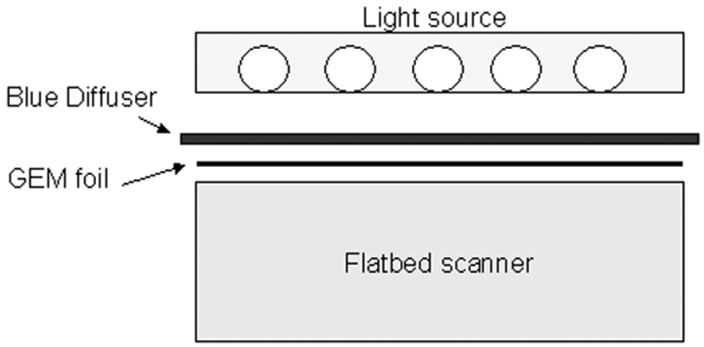

FIGURE 3.5. A schematic presentation of the scanning setup.

Even less could be said about general quality of the hole pattern of the foils. For example, the COMPASS experiment at CERN used a criterion of $\pm 2.5\mu$m around the mean diameter of the holes as acceptable [**3**]. They reported a gain uniformity of 15 %. The inhomogeneity of the size of the holes does affect the performance of the detector as discussed in chapter 4, but no studies on the effects of the shape of the holes have been done so far.

An optical scanning system was developed to find and record the etching defects of the T2 GEM foils. A schematic presentation of the system is shown in Figure 13. It was found that the setup was able to measure the sizes of the GEM holes and the pitch of the hole pattern. Even though no criterion for inhomogeneity of the holes was imposed in the QA process, the data could be used in the forthcoming research on the GEM foils themselves.

Direct inspection of the T2 GEM foils scans was not practical due to the large number (c.a. 1.8 million) of holes in each foil. Thus an automated technique was developed to find etching defects and to monitor the hole size distribution over the active GEM surface. The foils were scanned from both sides with Epson perfection 4180 Photo -scanner. Background lighting was provided through a blue diffuser to have color separation between reflected and transmitted light. Background light was used to find holes that were insufficiently etched and therefore blocked. The whole setup was located in class 100 clean room.

The scanner had a reported resolution of 4800 dot per inch (dpi), or a pixel size of about 5 μm x 5 μm. A calibration of the system with USAF 1951 1X calibration standard revealed, however, that real resolution in line pairs per mm (lp/mm) was less than reported. The resolution of the scanner varied over the x-axis from center (40 lp/mm) to worst on the right edge of the scanning area (18 lp/mm). Furthermore, the resolution was systematically worse in lateral than in vertical direction, probably due

to the optics of the line camera of the scanner and the way the image was supersampled in vertical direction only.

A resolution of 2400 dpi was decided to be used based on the aforementioned resolution issues and on the need to keep the file size below 2 GB due to internal memory limit of the scanner. With scanner resolution of 2400 dpi, each scan was about 1.2 GB in size and resolution varied from 32 lp/mm in center and left edge to 12.7 lp/mm in the far right edge of the scanner. As each foil was scanned from both sides, six images were acquired per detector. Some 300 scans were made in total amounting to roughly 360 GB of images.

Altogether the performance of the system was found to be adequate for its intended use. In addition to being able to locate etching defects and blocked holes, a good measure of the uniformity of the hole diameters could be achieved. The diameter of the holes was calculated from the area, in pixels, of the holes. On a good foil, a standard deviation of the areas of the holes was around 3 pixels, roughly equivalent to a standard deviation of about 5 μm in diameter, falling within the bounds of the tolerances reported by the manufacturer of the foils. In Figure 3.6, a 2D area histogram of the mean area of the holes is shown. In the plot the mean area of all of the holes is subtracted from the local mean to better visualize the small variations. The foil is scanned three times. Once in upright position, a second time rotated by 180°, and finally in upright position without the background light.

However, the scanning setup had its limitations. The resolution was not sufficient to separate holes in the copper, or outer holes, from the hole in the polyimide at the narrowest point of the double conical hole. Furthermore, due to the optics of the scanner, the viewing angle became inclined towards the edges of the scanning plane. To overcome these limitations a new scanning system, described in chapter 4, was developed. Some of the 13 spare detectors were scanned with the new system.

4. Testing

The gas gain and energy resolution of T2 GEM detectors were measured over all of the active area, separately for strips and pads. All the 17 readout sectors were tested in each GEM detector. All the 120 pads or 128 strips were connected to measure a full sector at a time. In the test, the whole readout sector was evenly irradiated with an ^{55}Fe source to get an estimate of the gain uniformity over the sector, readily visible in the width of the peak. The Full Width at Half Maximum (FWHM) resolution of the ^{55}Fe peak was around 25% for the average detector. A single ^{55}Fe-spectrum and a measurement of energy resolution as a function of operating voltage done with a collimated source is shown in Figure 3.7.

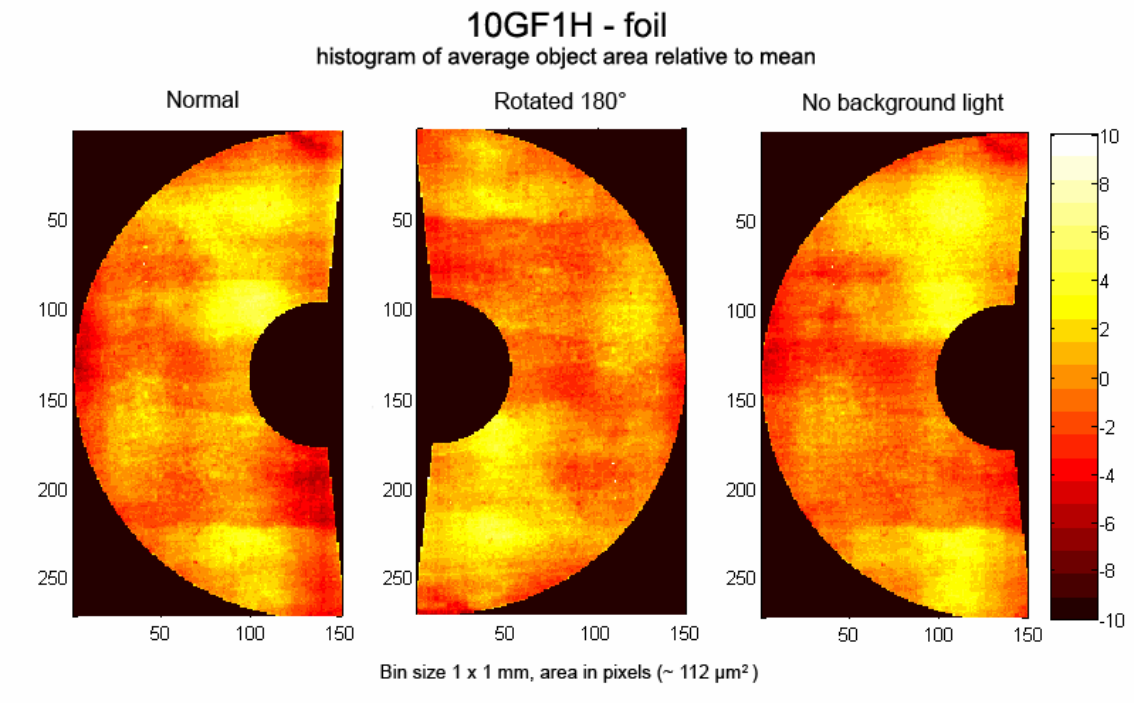

FIGURE 3.6. 2D histogram of the difference between average area of the holes in a bin relative to mean area of all holes in the foil. Foil HG10G scanned normally, rotated 180° and again without the use of background light. Unit of area is pixel. Bin size of the histogram is 1 mm by 1 mm.

Some detectors showed behavior that diverged from that of the others. The energy resolution of some sectors was found to be significantly worse than expected and, in some cases the peak was seen to form multiple maxima. No explanation to this behavior was found, but the effect could be diminished by irradiating the abnormal sector with high rate of x-rays (^{241}Am source). A single exceptionally bad detector, one that exhibited a factor of four difference in gas gain over 10 cm of surface, was reserved for further experimentation. The gas gain could be temporarily fixed by introducing water vapor in to the measurement gas. The difference in gain gradually re-emerged during 5 days of operation with dry gas. That particular detector was not installed into T2.

The gain variation behavior was observed only in some detectors, in different areas of the detector and depending on the irradiation rate and water content of the gas. Thus, it was concluded that it originates from GEM foils rather than from a flaw in the design of the detectors. It was impossible to correlate this gain variation with scans of the foils, though, even if some suspicious structures in the hole diameter maps could be identified (Such as the sharp decrease of hole size in the lower right part of the left

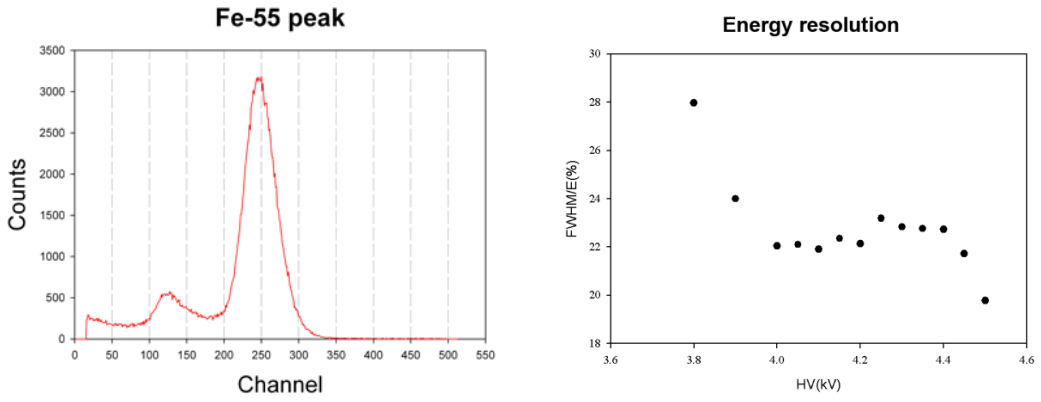

(a) (b)

FIGURE 3.7. The measured 6 keV ^{55}Fe peak shown in arbitrary units and the FWHM energy resolution as a function of the operating voltage.

image in Figure 3.6). Usually, the irregular behavior was seen in the first three or the last three pad sectors of the detector. (see readout sector map in Figure 3.3). This experience acted as further incentive for building the new scanning setup, described in Chapter 4.

Scanning of gas gain versus operating voltage was extended up to gains of 50000 – 100000, i.e. a magnitude higher than the nominal 8000. Testing for detector stability at the operating conditions was assigned a high priority. After testing for gain and energy resolution, the detectors were left at the nominal voltage (4.15 kV) for several days, normally at least for a week, to ensure a stable operation under normal running. The detectors were exposed to low rate irradiation from a ^{55}Fe source during the stability testing. No discharges were tolerated during the stability testing.

5. Results of T2 GEM Detector QA

Out of the 53 detectors built, 6 were rejected during the quality control. Two of the detectors had irreparable short circuits inside the chamber, two had frequent discharges at operating voltage and two had irreparable external discharges. Of the 40 GEM detectors installed at T2 telescope, five detectors had short circuits during the first months of operation, three of which were replaced with spare detectors. On four of the detectors, two external HV sectors had short circuited. The fifth detector had a single shorted internal sector. In all cases, failures occurred during the low luminosity runs with low center of mass energy. The rest of the detectors operated, with no discernible loss of performance, to the end of the 2012 run. This behavior

suggests that the short circuits were caused by concrete defects in the five detectors rather than by accident.

Thus, although the overall performance of the T2 GEM-detectors assembled at Helsinki was in the acceptable level, it was clear that a more accurate QA procedure should be implemented in the manufacturing process of MPGD.

CHAPTER 4

Optical Scanning System

1. Description

A large area scanning system was developed in the Detector Laboratory at Helsinki. The experience with the GEM foil scanner setup used in the quality assurance of T2 GEM detectors was capitalized in the design of the new scanning system. The system, described in detail in Publication II, was designed for optical scanning of significantly larger structures than the old system. The scanner table is suitable for GEM foils up to 95 cm by 95 cm in size. The resolution of the device was chosen such that it would be possible to simultaneously measure the hole in the copper electrode (the outer hole) and the more narrow hole in the center of the hourglass-like profile (the inner hole) of a double mask GEM foil.

The Optical Scanning System (OSS), provided by Optofidelity Ltd., consists of a three-axis precision positioning table, a 9 megapixel camera, a light table for background illumination and a ring light setup for foreground lighting. The OSS is shown in Figure 4.1. The camera is equipped with 1 x magnifying telecentric optics. The size of the imaged area is roughly 6 mm by 4.5 mm, so that a single pixel in the image is 1.75 μm by 1.75 μm. There is an option to use 0.32 x magnifying telecentric optics for coarse but faster imaging with an image area of 18 mm by 13.5 mm and a pixel size of 5.25 μm by 5.25 μm. This optional optics setup has not, however, been used in this work and the text is referring to the main optics.

Resolution of the system is measured to be 144 lp/mm in both blue and green channels and 128 lp/mm in red channel, using USAF 1951 1X calibration standard. The width of the optimal focal distance for the lens is 200 μm when studying objects less than or equal to 47.1 μm in size. Originally, the system had a laser range-finder to provide distance information for the focusing. However, the laser measurement proved to be unreliable when scanning highly reflective foils. Thus, the laser was replaced with an autofocus algorithm. The optimal focal distance is decided by the algorithm by comparing the sharpness of successive images taken with small displacement in the of the z-direction.

FIGURE 4.1. The optical scanning system.

The accuracy of the movement of the system, as given by the manufacturer, Optofidelity Ltd., is under 100 μm over the full scanning area in XY-plane, with a repeatability of less than 10 μm. In practice, however, the standard deviation of the error of the movement of the table between successive partly overlapping images was measured to be 2.7 pixels in x- and 3.0 pixels in y-direction, or 4.7 μm and 5.3 μm, respectively. The maximum speed of the x- and y-axes is 5 cm/s.

The scanner is controlled with a Labview program that takes care of the movement of the xyz-robot, the optical focusing and the defect analysis described in Publication IV. A separate analysis software, designed to run online with the scanner, was developed to perform accurate large area image analysis and processing of the results. The analysis software is described in Publication V.

2. Performance

The run settings for the scanner system for different foils vary from foil to foil as described in Publications III and V. Some foils reflect light in a diffuse way (matt), whereas others have specular reflection (mirror). The top row of Figure 4.2 is taken from a diffusely reflecting foil, the three others are from a mirror foil. In addition to the variable reflectivity, the foil surface is often textured with scratches, dust and oxidation or chemical residue.

The optimal settings for the scanner for each type of GEM foil are determined iteratively by tuning the exposure and the foreground lighting in order to to produce images that have clear separation between the features of the image. After the initial setup, the exposure time is fixed and the analysis software parameters are tuned to find the features. Setting up a scan of a foil can then be quickly done in the beginning

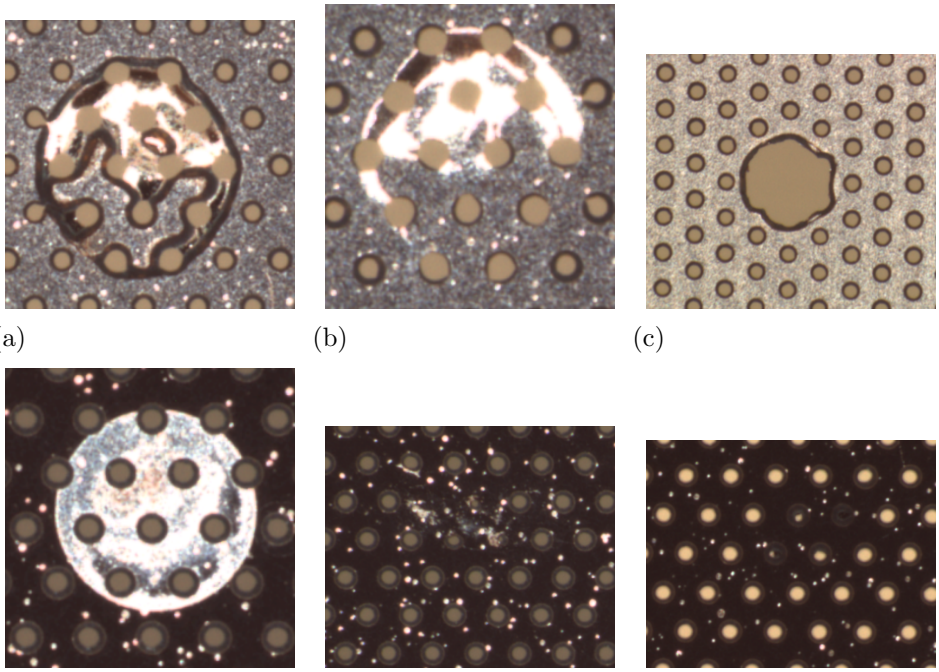

FIGURE 4.2. Sample pictures of different types of defects taken with the optical scanning system. (a) and (b) show a flaw formed by overetching of both the copper and the polyimide layer on one side of the foil. This can be seen also on the other side due to the bending of the copper surface. In (c) the overetching has removed both of the surfaces. In (d) some solvent is left on foil surface. In (e) and (f) the etching has been incomplete on one side of the foil creating small or blocked holes to this area.

of the scan by adjusting the foreground intensity. This is done by comparing the histogram of the image to the histogram of the reference image used in setting up the analysis software.

Previously, in case of big differences in the reflectance of foils, such as mirror and matt foils, separate setups of the analysis software were saved and used when needed. This is no longer necessary, though, as further modification to the optics was done. With the new inline lighting setup both reflective and matt foils can be scanned with the same settings.

3. Analysis Software

3.1. Description

The optical scanning system was designed to measure the diameters of inner and outer GEM holes. Thus, although defects in GEM foils would have to be found and

recorded, the performance of the scanner was designed to reach the requirements for accurate measurement of the holes. The system will be used as an essential part of the QA procedure in the assembly of GEM detectors and is expected to be continuously used when the production is ongoing.

An obvious challenge with the high resolution imaging over nearly a square meter area with the OSS, is the overwhelming amount of data generated by the system. A single full area scan takes roughly 700 GB of storage, placing rather severe limits on the storage time of the image data under continuous use. The amount of data after the analysis is not insignificant either: a foil of the size of the full scanning area would contain about 58 million holes. If the measurement of inner and outer hole was made to each hole from both sides of the foil, it would add up to 230 million individual measurements. The data alone would take almost 2 megabytes per recorded parameter when stored in floating point precision.

Another practical challenge in the analysis of the images of the optical scanning system is the huge variation between the images. The high variation in the surface properties of the individual GEM foils sometimes makes a careful adjustment of the lighting necessary before the scanning. In addition, sometimes multiple scans of an individual foil have to be taken before an adequate quality of the images is achieved. This is seriously challenging situation in detector production, when a large number of foils must be scanned in a short time before the assembly. Some of the later modifications to the optical scanning system, especially the autofocusing algorithm and the inline lighting, were made to mitigate the high variability of the images.

There was occasionally detrimental variation in the lighting within individual reflective foils due to waviness of the foil, as can be seen in Figure 4.3. Especially, in the case of large foils the waviness in the foil, combined with slight tilting of the scanner linears and the light table, could lead to large scale bands of over- or underexposed foreground. The banding was mostly seen in large framed foils, where the foils were visibly sagging in their frame. This variation proved to be especially difficult for the recognition of the outer holes.

In the end, the analysis software had to be flexible enough to compensate for at least some of the variation in the image quality. The software was designed to have a modular structure to enable easy changing of algorithms for each phase of the analysis process, controlled by a recipe file that could be tuned to optimize the performance.

The high storage space requirement of the image files lead to a solution in which the images could be deleted after they are analyzed, while the scanning was underway. A data reduction of roughly a factor of 40 is achieved. To take full advantage of the data reduction, the analysis has to stay up to the speed of the scanning. The time

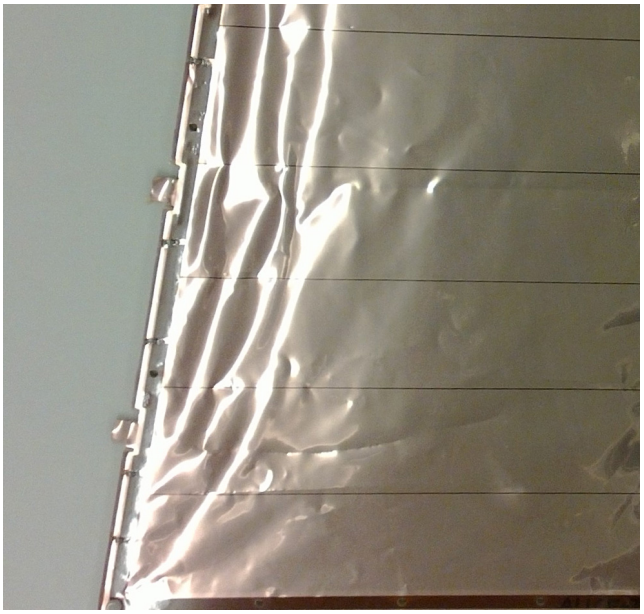

FIGURE 4.3. A framed GEM foil with waviness.

taken to analyze a single image is dependent on the complexity of the filters and algorithms specified in the recipe and can vary from seconds to tens of seconds per image. A close to linear speedup is achieved by running the analysis of several images on different cores of a multicore processor. In practice the bottleneck for the speed of analysis in the current realization of the setup is the transfer time of the images from the network drive to the computer performing the analysis.

After the analysis of the features of the GEM foil, the data is aligned, or stitched, image by image to correct for the error in location introduced by the variation of the step size of the robot. The accuracy of the movement of the scanning system between two neighboring images is of the order of 5 microns, well below the periodicity of the pattern of the holes on the GEM foils. This simplifies the stitching process and keeps the storage and time footprint of the stitching conveniently small. The stitching is further simplified by the fact that the movement of the robot is very linear and that the rotations and the shear of the images can be ignored in the stitching.

Small random rotations between neighboring images were found, though. This was most likely due to small rotations in the movement of the camera along the z-axis during the image focusing process. The rotations caused a random shift of a few pixels between neighboring images which in turn introduced an error on the stitching. Due to this error, the centroids of the holes, measured from both sides, did not exactly match each other. A histogram of the magnitude of this shift in the centroids, measured

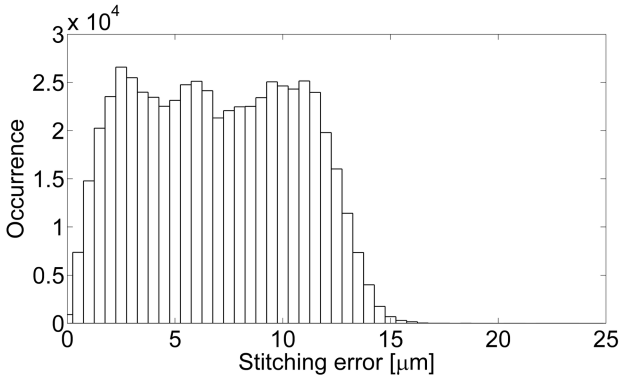

FIGURE 4.4. The error of the stitching of a 10 cm by 10 cm foil, measured by comparing the distance of the centroids of each hole measured from different sides of the foil.

from the inner holes, is shown in Figure 4.4. For a 10 cm by 10 cm foil, the shift is less than the radius of an inner hole.

Once the foil is stitched, the data can be used to fit both sides of the foil together to determine the real geometry of the individual holes. The precise measurement of the geometry of each GEM hole opens a direct way of studying the behavior of GEM detectors, especially when combined with detailed dynamical simulations.

3.2. Performance

The optical scanning system makes it possible to gather statistics of a large number of holes over large area instead of sampling on random locations. The statistical distribution of the characteristics of the foil in a local neighborhood can describe the foil performance more accurately than an exact measurement of a small subsample of the holes. One can readily see from Figures 4.5 and 4.6, that the variation is localized and could affect the uniformity of the detector response even if the standard deviation of the diameters of the holes is only 1.3 μm, well within the specifications of the manufacturer ($\pm 5\mu$m). This was indeed proved in Publication V, where the local variation of the diameters of the holes was correlated with the variation of the measured gain of a GEM foil.

When comparing the diameters of inner holes measured from different sides of a foil, a minor difference in the mean size of the holes is seen. The distribution of the Top diameter minus the Bottom diameter of each inner hole for a foil (foil 1 in Publication V) is shown in Figure 4.7. The mean value of this distribution is expected to be zero, but it was found to vary, with a standard deviation of 0.34 μm (calculated from the similar distributions of all of the 5 foils that were scanned). This uncertainty in diameter is probably due to minor differences in the lighting of the images which

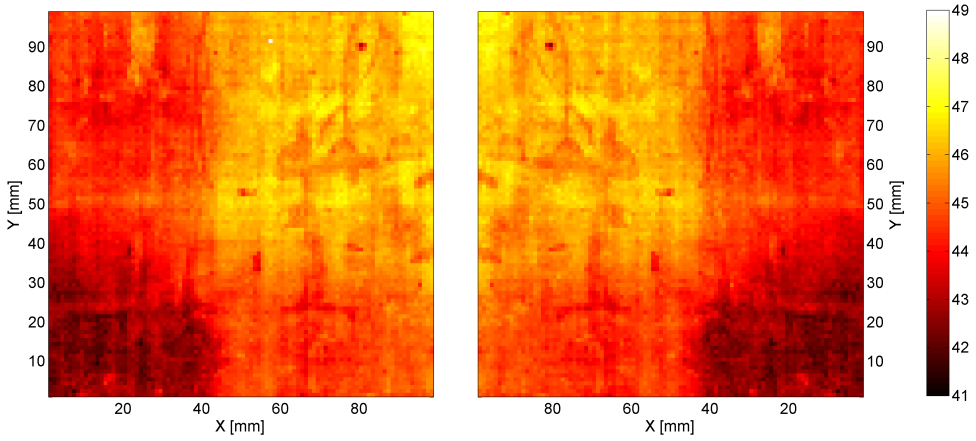

FIGURE 4.5. 2d-histograms of the inner diameter of the holes in a single CERN standard GEM foil measured from both sides of the foil. The size of the bins is 1 mm^2.

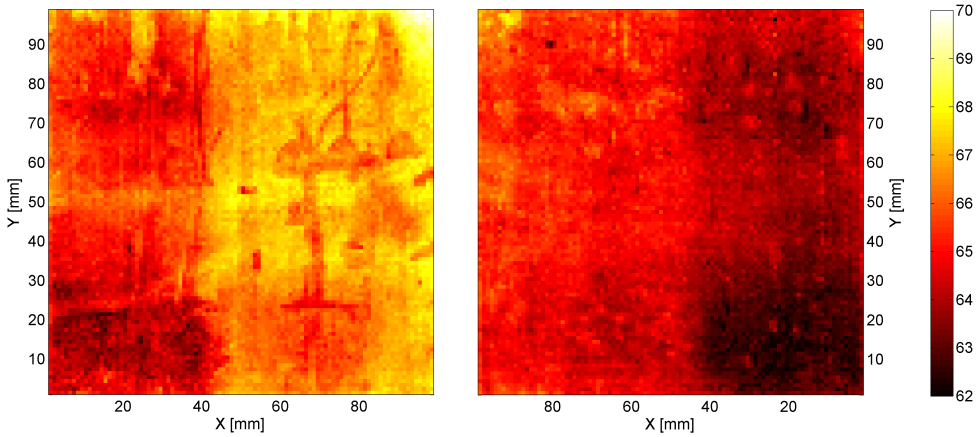

FIGURE 4.6. 2d-histograms of the outer diameter of the holes in a single CERN standard GEM foil measured from both sides of the foil. The size of the bins is 1 mm^2.

affects the edge detection algorithm when measuring the thin transparent polyimide inner boundary. This was understood as a systematic uncertainty of the diameter measurement.

Outer holes could not be measured in a similar way, but such offset was not found in the outer hole data when comparing two scans from the same side of a foil. Relative differences of the diameter of the holes within a single scan of the OSS can be measured with an uncertainty of 0.5 μm when using the ellipse fitting method presented in

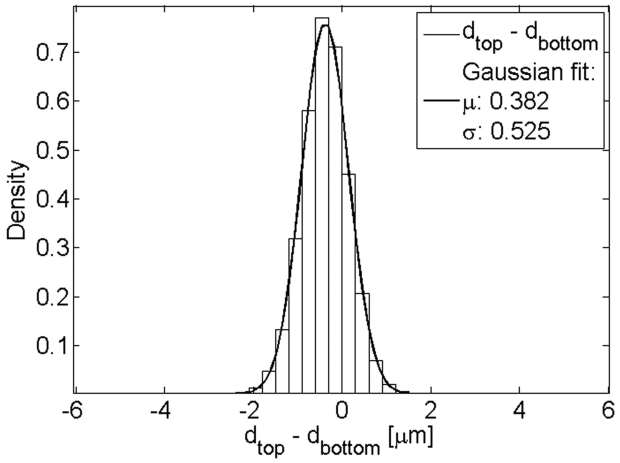

FIGURE 4.7. The difference between the inner diameters of each hole measured from opposite sides of a CERN standard GEM foil.

publication V. The error on the measurement is on the scale of the mean free path of electrons in gas under normal temperature and pressure. The uncertainty of the pitch measurement is 0.3 μm. The analysis software can be used to accurately characterize the outer and the inner hole diameters and the pitch of the GEM foils, all properties relevant to the performance of the foils.

The shape of the holes can likewise be evaluated from the data. The amount of exposed polyimide, or the rim width, can be estimated from the difference between the radii of the inner and outer holes. Furthermore, the degree of ellipticity can be evaluated directly from the difference between the minor and major axes of the ellipse fit. Clearly deviating values of these parameters may indicate problems with the foil manufacturing process, such as mask alignment error. An example of the measurement of the rim width, ellipticity and offset in the centroids of inner and outer holes for two different GEM foils is shown in Figure 4.8. Here foil 2 is fairly typical foil, but the holes in foil 3 are slightly elliptical and off-centered, probably due to mask alignment error.

3.3. Correlation of Hole Size and Gain

Gain mapping was made to three standard CERN double mask foils to correlate the variation in the sizes of the holes to the measured variation in the gas multiplication. Two different measurement setups were used. A high precision setup (setup 1) was utilized with a low gain over one of the foils, foil 2, and a lower precision setup (setup 2) with high gain and different gas mixture for foils 1, 2 and 5. The latter setup was used

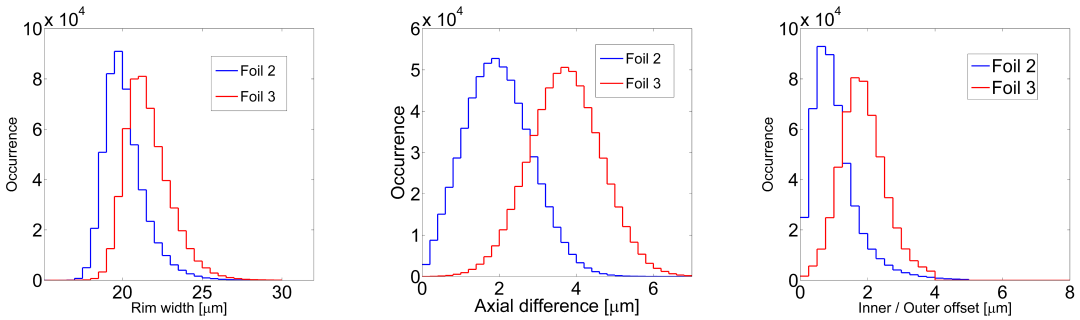

(a) (b) (c)

FIGURE 4.8. Histograms of the rim width (left), the difference between the ellipse axes (middle) and the offset (right) of the centroids of the inner and outer hole for two CERN standard foils.

to see if any correlation would hold with a radically different setup and with other foils. The details of the measurements are described in Publication V.

A 2-dimensional map of the diameters of the holes was calculated and compared to a detailed gain map of the detector. It was found that the diameter of the holes correlates inversely with the gain of the foil. This is expected to a degree, as shown already in reference [**19**]. A simplified prediction of the gain variation, based on the inverse linear correlation of the diameter of the holes to the gain, was calculated for each foil. The relative variation of the prediction, basically just the hole diameters inverted and multiplied together bin by bin, did reflect the actual gain variation measured with setup 1. The measured gain map and the prediction, normalized to the same mean gain, is shown in Figure 4.9(a) and (b), respectively.

It was found, however, that the gain prediction was less accurate on one of the foils measured with setup 2. The correlation of the prediction against measured gain for all measurements is shown in Figure 4.10. The measurement with setup 1 is drawn with blue crosses. Two of the foils measured with setup 2 (i.e. 2a) seem to be predicted rather well. On the other hand, one foil (i.e. 2b) does not show as clear correlation in the higher end of the gain. The diameter map of this foil (i.e. foil 5 in Publication V) is shown in Figure 4.5 for the inner holes and in Figure 4.6 for the outer holes. As can be seen from the map, this particular foil has unusually small holes on one corner of the foil. The prediction probably fails because of the saturation effect described in Chapter 2.

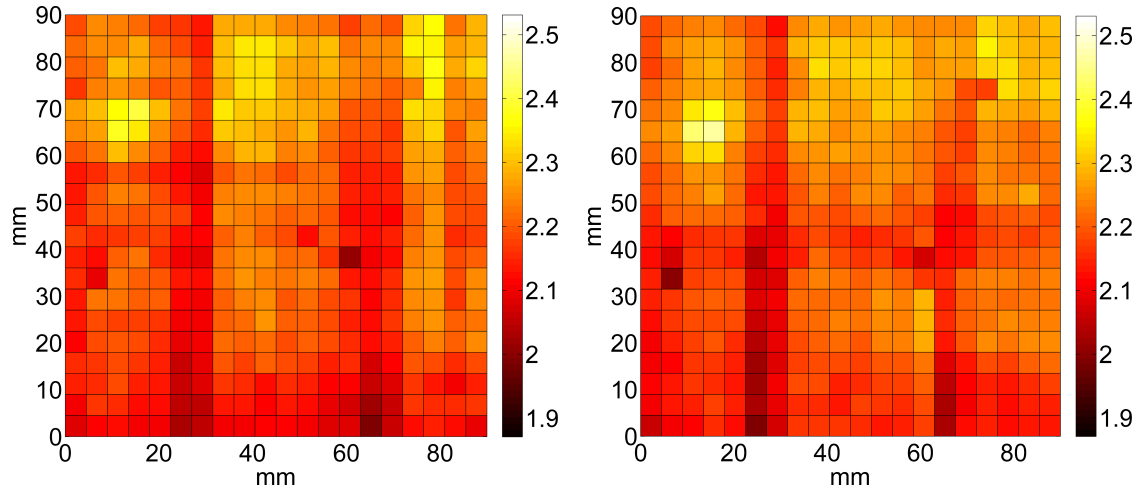

(a) (b)

FIGURE 4.9. The measured (a) and predicted (b) gain for the foil measured with setup 1.

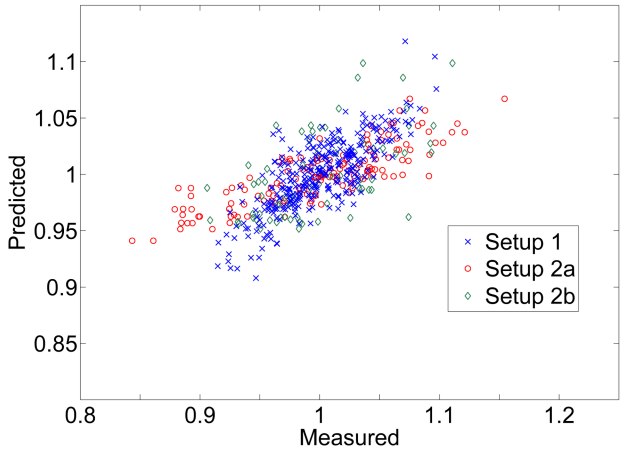

FIGURE 4.10. The predicted gain, based on inverse linear correlation of the diameter, against the measured relative gain. The measurement with setup 1 is drawn with crosses and the measurement with setup 2 for two normal foils and the foil with small holes is drawn with circles and lozenges, respectively.

3.4. Calibration of the OSS

Whereas the relative variation in the size of the holes can be reliably measured with OSS, the absolute accuracy of the measurement cannot be determined without calibration. Publication VI describes a calibration of the system, using micro-manufactured silicon calibration samples with highly specular surface, much like that of a reflective GEM foil. Three designs of microfabricated transfer standards [**24**] with geometry

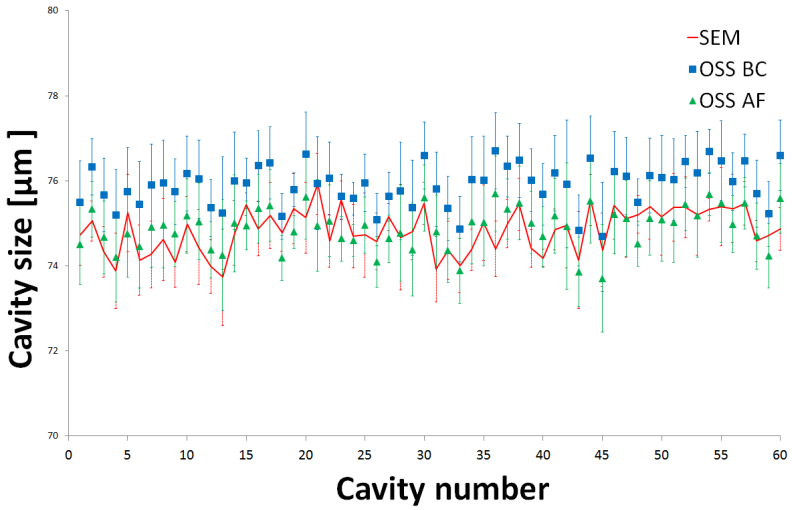

FIGURE 4.11. The 60 TS#1 compared to the SEM before (BC) and after (AC) the calibration of the OSS.

similar to that of GEM holes was used for the lateral calibration of the system. The calibration is based on data collected with two of the three standards. The main difference between the two designs is in the TS geometry. The TS#1 replicates the outer contour of the GEM foil hole while both the inner and the outer contour are replicated in TS#2.

The system calibration factor was extracted by scanning the two TS by Scanning Electron Microscope (SEM) and then by the OSS. For the calibration, altogether 60 cavities from TS#1 and 45 cavities from TS#2 were selected. The diameter of each cavity was measured and the obtained results were compared. The calibration factor was defined according to ISO and UKAS reglementation [**25**, **26**]. The SEM measurement of the diameters of the cavities, together with the raw and calibrated measurements with OSS are shown in Figures 4.11 - 4.13.

The calibration is only valid for the mirror foils, though. After the inline lighting upgrade of the OSS, a single calibration could be used for mirror and matte foils alike. The small variation of the diameter measurement discussed above, caused by minor differences in the lighting and the nonlinearity of the camera response underlines the sensitivity of the measurement. For example, a change in the preprocessing algorithm can lead to a systematic change in the measured diameters. Furthermore, the calibration factor for the diameter measurement depends on whether the measured contour lies in a transition from light to dark area (inner hole) or vice versa (outer hole). A proper calibration has to be performed to each measurement setup to make certain that the results are comparable to earlier measurements.

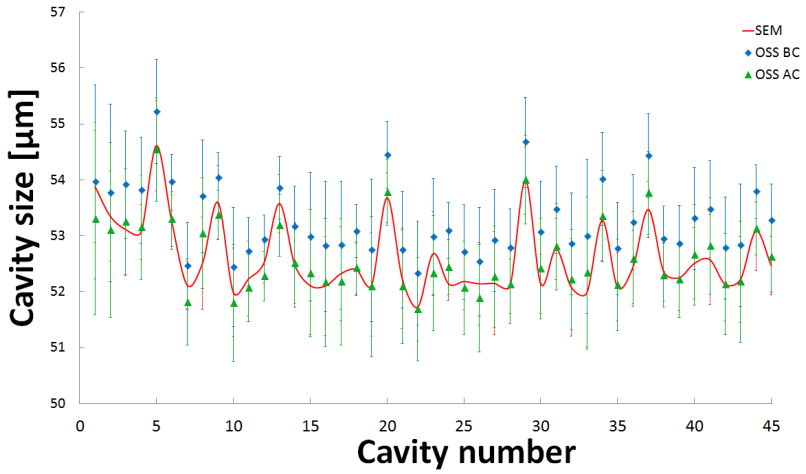

FIGURE 4.12. The 45 inner cavities from TS#2 compared to the SEM before (BC) and after (AC) the calibration of the OSS.

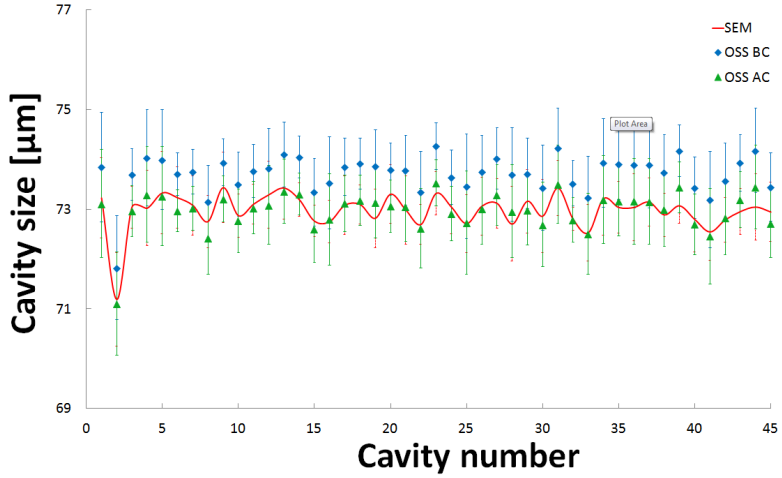

FIGURE 4.13. The 45 outer cavities from TS#2 compared to the SEM before (BC) and after (AC) the calibration of the OSS.

CHAPTER 5

Discussion

QA is an essential process in the production of GEM detectors. Each component of the detector has to pass the previously set quality requirements. Furthermore, the production process has to be carefully recorded in order to monitor the procedure. In addition to checking the basic functionality of the detector, such as gas leaks, HV-system isolation, gain characterization etc., some GEM foil specific steps were found useful during the T2 GEM detector assembly.

Even though a GEM detector is a relatively robust detector, a single GEM foil is easily ruined if it is exposed to dust or contaminants, such as a droplet of glue. Each foil can be damaged until the detector is sealed. Even with the cleanliness of the T2 detector assembly environment in a class 100 cleanroom, accidents did happen while handling the foils. These were not always noticed during the incident. Leakage current test proved to be the most useful single test of the performance of a GEM foil during the T2 assembly. The decision of performing the leakage current testing on several phases of the T2 assembly process saved time and resources on several occasions as foils were broken during the assembly process.

In addition to leakage current testing, another electrical test can be made to the GEM foils. CERN Microelectronics laboratory, the largest GEM foil manufacturer at present, routinely tests the foils by increasing the voltage over the foil up to 600 V, near the limit of spontaneous sparking. This procedure can quickly blast away some of the dust attached to the foil, compared to slowly burning the dust during the leakage current test or normal operation of the GEM detector. The procedure serves also as a stress test to the foil. If the foil has a defect that will cause an electrical breakdown, it will be immediately visible as there will be sparks in this weak spot. Even if such a test was not used in the T2 assembly, it could be useful for new foils, before other testing is performed.

The optical analysis of GEM foils is a new useful method of GEM foil QA. Mapping of the defects that are formed in different manufacturing stages of GEM-foils is an important phase when determining the suitability of an individual foil for assembly. There is evidence that defects of certain type and size might expand and generate

additional damage to the GEM-foils under irradiation, as described in Publication IV. With an optical scanning system, these defects can be recorded for further analysis.

Difference in the average size of the holes between two foils of a detector does not necessarily compromise the performance of a GEM detector. If necessary, the differences in gain of each foil can be compensated by changing the voltage of the detector as long as the discharge probability for any of the foils does not increase dramatically. On the other hand, variation in the sizes of the holes within a single foil has been shown to influence the uniformity of the detector response. Some insight to the nature of the correlation between the variation of the sizes of the holes and the gain variation of the foil is given in Publication V. The exact behavior of the gain as function of the size and shape of the hole and the field setup cannot yet be modelled accurately. Some promising results have been presented using dynamic charging-up simulations with the Garfield++ simulation library coupled with electric field calculations by a Finite Element Method (FEM) program, as is shown in references [**20**, **21**].

An important application of the optical analysis of GEM foil QA is to monitor the variation of the characteristics within each foil. The suitability of a foil can be evaluated using a relevant statistical quantity, such as the standard deviation, of the features. Moreover the operation of a foil can be estimated in conjunction with the other foils of a multi-foil detector. In this way it is possible to prevent the stacking up of foils that exhibit unwanted behavior in the same area of the detector in applications that have strict requirements on the homogeneity. Thus the yield of the detector manufacturing process may be increased by choosing each foil in such a way that the homogeneity criterion is met.

CHAPTER 6

Summary

A thorough QA procedure was applied in the production of GEM detectors for the TOTEM T2 telescope at CERN, spanning from the arrival of the components to the performance testing of each detector module. All in all the production of the T2 detectors was a success. The T2 telescope was operational and took data during LHC running, when the luminosity allowed it, up until the long shutdown in 2013. It was left in place inside the Forward Calorimeter of CMS to be used on forthcoming special physics runs.

During the operation of T2, five of the GEM detectors had short circuits in one or more HV sectors. The short circuits mostly happened in external sectors farthest from the beam. The short circuits occurred during the lower energy and lower intensity runs in the first years of the operation of the LHC, in an area of the detector that had the smallest particle flux. The pattern of the short circuits was not fully understood. Even though several HV sectors out of 480 were lost due to short circuits during the running of the experiment, the functionality of the telescope as a whole did not suffer, largely due to the redundancy given by the 10 detector planes per quarter of the telescope.

Optical scanning methods were developed for the QA of the TOTEM T2 assembly. The results of the optical scanning were not used to disqualify GEM foils from production, largely because the effect of anomalies in the foils was unknown at the time. However, feedback was given to the foil manufacturers based on the results on hole uniformity and defects. The experience with the optical QA method lead to the development of new scanning system and methodology for forthcoming GEM production tasks at the Detector Laboratory of the Helsinki Institute of Physics and the Department of Physics at the University of Helsinki. The next generation optical scanning system was designed for high resolution scanning of GEM foils up to 95 cm by 95 cm in size. It was originally targeted for the QA procedures of the GEM-TPC beam diagnostics detectors for the Super-FRS experiment at FAIR, but was taken into use also for the QA of the GEM foils of ALICE TPC upgrade project.

The analysis software for the optical scanning system was developed side by side with the hardware and control software of the system. The software was optimized to perform with high fidelity together with the scanner. The performance of the

software was studied thoroughly and the hole-size measurement was calibrated before taking the scanner into use in the QA of the GEM detectors of Super-FRS and ALICE experiments.

It was found, that in addition to recording defects of the GEM foils, the optical QA could be used to provide further insight to the connection of the geometry of the individual GEM holes to the performance of the detector. Especially, the high resolution measurement of the individual GEM holes provides a way to qualitatively estimate the gain homogeneity of the foils. The relation of the homogeneity of the gain and the variation of the size of the holes makes it possible to use the size information constructively during the QA, when deciding which foils will be stacked into each detector.

Bibliography

[1] F. Sauli, "GEM: A new concept for electron amplification in gas detectors," Nucl. Instrum. Meth. A **386** (1997) 531.

[2] B. Ketzer, Q. Weitzel, S. Paul, F. Sauli and L. Ropelewski, "Performance of triple GEM tracking detectors in the COMPASS experiment," Nucl. Instrum. Meth. A **535** (2004) 314 [Erratum-ibid. A **648** (2011) 293].

[3] B. Ketzer, M. C. Altunbas, K. Dehmelt, J. Ehlers, J. Friedrich, B. Grube, S. Kappler and I. Konorov *et al.*, "Triple GEM tracking detectors for COMPASS," IEEE Trans. Nucl. Sci. **49** (2002) 2403.

[4] S. Dalla Torre, "MPGD developments: historical roadmap and recent progresses in consolidating MPGDs," JINST **8** (2013) C10020.

[5] F. Murtas, "Applications of triple GEM detectors beyond particle and nuclear physics," JINST **9** (2014) C01058.

[6] V. Berardi *et al.* [TOTEM Collaboration], "TOTEM: Technical design report - Addendum. Total cross section, elastic scattering and diffraction dissociation at the Large Hadron Collider at CERN," CERN-LHCC-2004-020.

[7] M. Alfonsi, G. Bencivenni, P. De Simone, F. Murtas, M. Poli Lener, W. Bonivento, A. Cardini and D. Pinci *et al.*, "The LHCb triple-GEM detector for the inner region of the first station of the muon system: Construction and module-0 performance," IEEE Trans. Nucl. Sci. **53** (2006) 322.

[8] B. Ketzer [GEM-TPC and ALICE TPC Collaborations], "A Time Projection Chamber for High-Rate Experiments: Towards an Upgrade of the ALICE TPC," Nucl. Instrum. Meth. A **732** (2013) 237 [arXiv:1303.6694 [physics.ins-det]].

[9] D. Abbaneo, C. Armagnaud, M. Abbrescia, P. Aspell, S. Bally, Y. Ban, L. Benussi and U. Berzano *et al.*, "GEM based detector for future upgrade of the CMS forward muon system," Nucl. Instrum. Meth. A **718** (2013) 383.

[10] K. : F. Archilli *et al.* [2 Collaboration], "Technical Design Report of the Inner Tracker for the KLOE-2 experiment," arXiv:1002.2572.

[11] M. Kalliokoski, F. Garcia, A. Numminen, E. Tuominen, R. Janik, M. Pikna, B. Sitar and P. Strmen *et al.*, "GEM-TPC Trackers for the Super-FRS at FAIR," Conf. Proc. C **100523** (2010) MOPD082.

[12] E. Rutherford and H. Geiger, "An Electrical Method of Counting the Number of α-Particles from Radio-active Substances," Proceedings of the Royal Society, London **A81**, 141 (1908).

[13] H. Schindler and R. Veenhof, "GARFIELD++ — simulation of tracking detectors," `http://cern.ch/garfieldpp`.

[14] H. Andersson, T. Andersson, J. Heino, J. Huovelin, K. Kurvinen, R. Lauhakangas, S. Nenonen, A. Numminen, J. Ojala, R. Orava, J. Schultz, H. Sipila, and O. Vilhu, "Analysis of compounds released from various detector materials and their impact on aging Characteristics of proportional counters," IEEE Trans. Nucl. Sci. **51** (2004) 5, 2110.

[15] S. Bachmann, A. Bressan, M. Capeans, M. Deutel, S. Kappler, B. Ketzer, A. Poluektov and L. Ropelewski *et al.*, "Discharge studies and prevention in the gas electron multiplier (GEM)," Nucl. Instrum. Meth. A **479** (2002) 294.

[16] G. Charpak, R. Bouclier, T. Bressani, J. Favier and C. Zupancic, "The use of multiwire proportional counters to select and localize charged particles," Nucl. Instrum. Meth. **62** (1968) 262.

[17] A. Oed, "Position Sensitive Detector with Microstrip Anode for electron Multiplication with Gases," Nucl. Instrum. Meth. A **263** (1988) 351.

[18] Y. Giomataris, P. Rebourgeard, J. P. Robert and G. Charpak, "MICROMEGAS: A High granularity position sensitive gaseous detector for high particle flux environments," Nucl. Instrum. Meth. A **376** (1996) 29.

[19] S. Bachmann, A. Bressan, L. Ropelewski, F. Sauli, A. Sharma and D. Mormann, "Charge amplification and transfer processes in the gas electron multiplier," Nucl. Instrum. Meth. A **438** (1999) 376.

[20] M. Alfonsi, G. Croci, S. Duarte Pinto, E. Rocco, L. Ropelewski, F. Sauli, R. Veenhof, M. Villa, "Simulation of the dielectric charging-up effect in a GEM detector," Nucl. Instrum. Meth. A **671** (2012) 6.

[21] P. M. M. Correia *et al.* [CERN RD-51 Collaboration], "A dynamic method for charging-up calculations: the case of GEM," JINST **9** (2014) P07025.

[22] V. Berardi *et al.* [TOTEM Collaboration], "TOTEM: Technical design report. Total cross section, elastic scattering and diffraction dissociation at the Large Hadron Collider at CERN," CERN-LHCC-2004-002.

[23] G. Antchev *et al.* [TOTEM Collaboration], "Measurement of the forward charged particle pseudorapidity density in *pp* collisions at $\sqrt{s} = 7$ TeV with the TOTEM experiment," Europhys. Lett. **98** (2012) 31002.

[24] A. Karadzhinova, M. Berdova, T. Hildén, J. Heino, R. Lauhakangas, E. Tuominen, S. Franssila, E. Haeggström, and I. Kassamakov, "Microfabrication of Transfer Standards for Calibration of Optical Quality Assurance System," Proc. 24th Micromechanics Microsyst. Eur. Conf. (2013).

[25] "ISO/IEC 17025 - General requirements for the competence of testing and calibration laboratories, 2nd." (2005).

[26] "M3003-The Expression of Uncertainty and Confidence in Measurement." United Kingdom Accreditation Service, (2012).